



# There is no general model for occlusal kinematics in conodonts

CARLOS MARTÍNEZ-PÉREZ, PABLO PLASENCIA, DAVID JONES, TEA KOLAR-JURKOVŠEK, JINGENG SHA, HECTOR BOTELLA AND PHILIP C.J. DONOGHUE

## LETHAIA



Martínez-Pérez C., Plasencia P., Jones D., Kolar-Jurkovšek T., Sha J., Botella H. & Donoghue P.C.J. 2014: There is no general model for occlusal kinematics in conodonts. *Lethaia*, Vol. 47, pp. 547–555.

Knowledge of conodont element function is based largely on analysis of morphologically similar P<sub>1</sub> elements of few comparatively closely related species known from abundant articulated remains. From these, a stereotypical pattern of rotational occlusion has been inferred, leading to the suggestion that this may represent a general model for ozarkodinid P<sub>1</sub> elements at the very least. We test the generality of this occlusal model through functional analysis of *Pseudofurnishius murcianus* P<sub>1</sub> elements which, though superficially similar to homologous elements in gnathodids, evolved their platform morphology independently, through a different mode of morphogenesis, and in a different topological position within the element. Our integrated functional analysis of several articulated clusters of P<sub>1</sub> elements encompassed physical and virtual occlusal analyses, constrained by microwear and sharpness analyses. All of the evidence supports an occlusal model in which the *Pseudofurnishius* P<sub>1</sub> elements occluded with the dextral blade located between the rostral face of the sinistral blade and the first cusp of the rostral primary process. In achieving this, the dorsal and ventral blades guided the opposing elements, and the rostral processes of both elements guided the final stages of precise occlusion. Spalling and microwear on the non-occlusal side of the element evidence malocclusion, requiring the complete separation of elements within the occlusal cycle. This occlusal cycle is entirely linear, orthogonal to the plane of attachment of the elements. Evidently, the rotational occlusal model is not general for P<sub>1</sub> elements, even for ozarkodinids, and it is likely that among conodonts occlusal kinematics are as disparate as element morphologies. Attempts to elucidate the diversity of occlusal kinematics and, therefore, feeding ecologies of conodonts will be repaid by an understanding of the role of this important abundant and diverse clade in Palaeozoic and Mesozoic marine ecosystems. □ *Conodont kinematics, digital occlusion, microwear and sharpness analyses.*

Carlos Martínez-Pérez [Carlos.Martinez-Perez@bristol.ac.uk], David Jones [david\_jones001@hotmail.com], Philip C.J. Donoghue [Phil.Donoghue@bristol.ac.uk], School of Earth Sciences, University of Bristol, Wills Memorial Building Queen's Road, Bristol, BS8 1RJ, UK; Pablo Plasencia [Pablo.Plasencia@uv.es], Hector Botella [Hector.Botella@uv.es], Department of Geology, University of Valencia, Dr. Moliner 50 Burjassot, 46100 Valencia, Spain; Tea Kolar-Jurkovšek [tea.kolar@geo-zs.si], Geološki zavod Slovenije, Dimičeva 14, 1001 Ljubljana, Slovenija; Jingeng Sha [jgsha@nigpas.ac.cn], State Key Laboratory of Palaeobiology and Stratigraphy, Nanjing Institute of Palaeontology and Geology, 39 East Beijing Road, 210008 Nanjing, China; manuscript received on 05/12/2013; manuscript accepted on 17/03/2014.

Conodonts are an extinct group of jawless vertebrates, the first in the vertebrate lineage to experiment in skeletal biomineralization, manifest as an array of tooth-like dental elements. Debate over the function of conodont elements was long inextricably linked to debate over the conodont affinity and so functional inferences were based on speculative hypotheses of homology to the teeth and spines of multifarious vertebrates and invertebrates. Ironically, the discovery of conodont soft tissue anatomy freed functional analysis from phylogenetic constraint. This was presaged by early attempts at inferring function by analogy to physically similar structures in unrelated organisms (Jeppsson 1979), assuming functional optimality of both conodont

elements and their analogues. However, attempts to elucidate conodont functional morphology based on the intrinsic properties of the elements began with Nicoll (1985, 1987) who, through occlusal analysis of artificial element pairs, was among the first to have considered seriously how elements would have interacted in life. Nicoll's analyses suggested that the elements did not occlude as do gnathostome teeth and, therefore, did not function as such. However, functional analysis of elements dissected from the articulated skeletal remains of single individuals demonstrated precise rotational occlusion comparable to the most sophisticated of mammalian dentitions (Donoghue & Purnell 1999a). The opposing P<sub>1</sub> elements are aligned by their long ventral processes

such that their dorsal processes are brought into precise rotational occlusion, before the ultimate separation of the elements to permit the input of unprocessed food materials and the output of their processed products (Donoghue & Purnell 1999a; Jones *et al.* 2012). This pattern has been corroborated by microwear analyses (Purnell 1995; Donoghue & Purnell 1999a,b; Jones *et al.* 2012; Martínez-Pérez *et al.* 2014) and demonstrated in the P<sub>1</sub> elements of all other species investigated, culminating in what has been considered a general occlusal model (Jones *et al.* 2012; Martínez-Pérez *et al.* 2014).

Although there have been great advances in analytical approaches to, and knowledge of, conodont element function, these have been based on the sum of analyses of a very small suite of closely related and morphologically similar conodont species, such as the blade-shaped *Ozarkodina* and *Wurmiella* (Purnell 1995; Donoghue 2001; Jones *et al.* 2012), and the molariform gnathodids *Idiognathodus* and *Gnathodus* (Purnell 1995; Donoghue & Purnell 1999a,b; Martínez-Pérez *et al.* 2014). Indeed, the gnathodids evolved from the *Ozarkodina* lineage, elaborating the morphology of the P<sub>1</sub> elements from simple blade dorsal ('posterior') and ventral ('anterior') processes to possess a dorsal molariform occlusal platform. It is perhaps not surprising, therefore, that functional analyses of these taxa have revealed common patterns of occlusal kinematics (Donoghue & Purnell 1999a; Jones *et al.* 2012; Martínez-Pérez *et al.* 2014). Testing the generality of this functional interpretation is limited because occlusal kinematics can be studied only in elements from articulated skeletal remains of single individuals, which are scarce and rarely occur in the abundance required for destructive analysis (e.g. Donoghue & Purnell 1999a). However, with the development of high-resolution, high brilliance tomographic methods (Donoghue *et al.* 2006), it is now possible to characterise virtually the morphology of elements in these rare articulated assemblages and subject their avatars to functional analysis (Jones *et al.* 2012; Murdock *et al.* 2013; Martínez-Pérez *et al.* 2014). This expands considerably the material available for investigation.

Thus, to test the general relevance of the occlusal model based in ozarkodinid conodonts, we undertook a functional analysis of the P<sub>1</sub> elements of *Pseudofurnishius murcianus*. The P<sub>1</sub> elements of *Pseudofurnishius* are morphologically similar to those of gnathodids, in that they are comprised of a free blade and a reduced molariform platform (Fig. 1). However, *Pseudofurnishius* evolved this morphology independently and in manner different

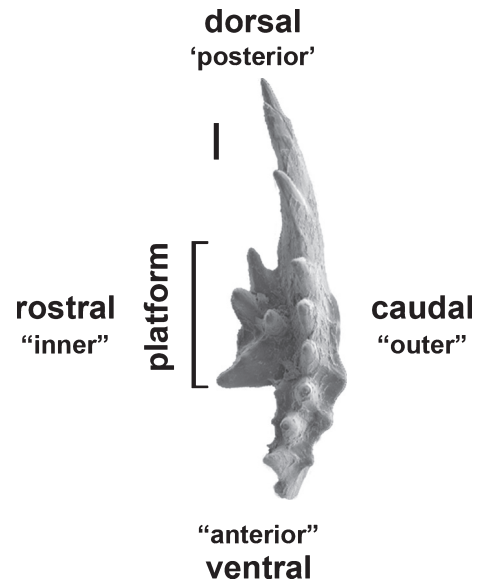


Fig. 1. Complete P<sub>1</sub> element of *Pseudofurnishius murcianus* showing the orientation and different morphological terms with the traditional notation in quotation marks. MGUV-19866. Libros, Iberian Range, Ladinian (Longobardian). Scale bar 50  $\mu$ m.

to the gnathodids. *Pseudofurnishius* develops its platform by adding primary and secondary lateral processes to form a complex morphology (the 'icrion' of Dzik 1991, 2006 or 'type A platform' of Donoghue 1998), contrasting with gnathodids, which develop their platforms through the lateral expansion of the blade itself (the 'platform' of Dzik 1991, 2006 or 'type B platform' of Donoghue 1998). Indeed, although *Pseudofurnishius* is a gondolellid and, therefore, a member of the same suborder Ozarkodinina as *Ozarkodina*, *Wurmiella* and the gnathodids, gondolellids are as distantly related to these taxa as is possible within the clade Ozarkodinina (Donoghue *et al.* 2008). Underlining this phylogenetic remoteness, the morphological similarity of *Pseudofurnishius* and gnathodid P<sub>1</sub> elements is entirely superficial because the *Pseudofurnishius* P<sub>1</sub> element is composed of a central platform and dorsal ('posterior') and ventral ('anterior') free blades, while the gnathodid P<sub>1</sub> elements are composed of a dorsal platform and ventral free blade. This represents one of the greatest differences in element morphology considered functionally hitherto and, thus, represents an effective test of the general occlusal model. To that end, we undertook an integrated functional analysis of *Pseudofurnishius* P<sub>1</sub> elements through sub-micron characterization of element morphology using the Synchrotron X-Ray Tomography Microscopy (Donoghue *et al.* 2006), before subjecting the resulting avatar to both physical (scaled 3D prints) and virtual occlusal analyses constrained by the results of a microwear analysis.

## Material and methods

Our study was based on both articulated clusters of elements and disarticulated elements. The studied articulated clusters of  $P_1$  elements come from single individuals of *Pseudofurnishius murcianus* from the Prikrnica locality, which is located north-west of the village of Moravče (Ladinian-earliest Carnian, Middle-Upper Triassic) in the Slovenian Basin of Central

Slovenia (see Krivic & Stojanovič 1978). The disarticulated  $P_1$  elements were obtained from the Calanda, Libros, Henarejos and Bugarra sections of the Iberian Range and from the Calasparra Section of the Betic Cordillera, eastern Spain (Ladinian, Middle Triassic) (see Plasencia 2009). The clusters include pairs of  $P_1$  elements that would have functioned together *in vivo* (Fig. 2). For the occlusal analysis and sharpness measurements, several clusters and isolated elements were characterized using synchro-



Fig. 2. Tomographic 3D models of *Pseudofurnishius murcianus*  $P_1$  elements clusters from Prikrnica locality, Central Slovenia. A, B, cluster GeoZS 559 with the occlusal pair in rostral (A) and caudal (B) views. C, D, elements from the articulated clusters in oral view, right (C) and left (D) elements. E, right, and F, left, elements in lateral (rostral) view showing the asymmetry of the platforms between the pair elements. G–K, broken cluster (GeoZS 546) of *Pseudofurnishius murcianus*. G–I, tomographic reconstruction in rostral (G), caudal (H) and dorsal view (I); J–H, elements from the articulated clusters in oral view, left (J) and right (H) elements. Scale bars: (A, B) 100  $\mu\text{m}$ ; (C, E) 115  $\mu\text{m}$ ; (D, F) 120  $\mu\text{m}$ ; (G–K) 75  $\mu\text{m}$ .

tron radiation X-Ray Tomography (srXTM), using the X02DA TOMCAT beamline at the Swiss Light Source, Paul Scherrer Institute (Villigen, Switzerland), using a 20× objective, exposure time at 14 keV of 130 ms, acquiring 1501 projections equi-angularly over 180°. Projections were post-processed and rearranged into flat- and dark-field-corrected sinograms, and reconstruction was performed on a 60-core Linux PC farm using a Fourier transform routine and a regridding procedure (Marone & Stampanoni 2012). The resulting volume has isotropic voxel dimensions of 0.36  $\mu\text{m}$ . Slice data were analysed and manipulated using AVIZO v.7.1 (VSG). 3D prints of the resulting models were created using a Stratasys Fortus 400mc printer. The approximately 150 times scale-enlarged physical models of the elements from the articulated clusters were used to inform our digital occlusal analysis in BLENDER v. 2.63 (<http://www.blender.org>). Finally, and following the methodology proposed by Jones *et al.* (2012) to identify the primary power stroke and hence inform the kinematic model, three-dimensional sharpness measurements of the ventral and dorsal edges of the blade denticles were acquired from the digital models in GEOMAGIC STUDIO v. 12 (Geomagic, USA). The different denticles of the blade were identified and numbered from ventral to dorsal, quantifying the diameter of a cylinder fitted in the denticle edges as a sharpness approximation (see Fig. 3 and Jones *et al.* 2012 for a detailed description of the methodology).

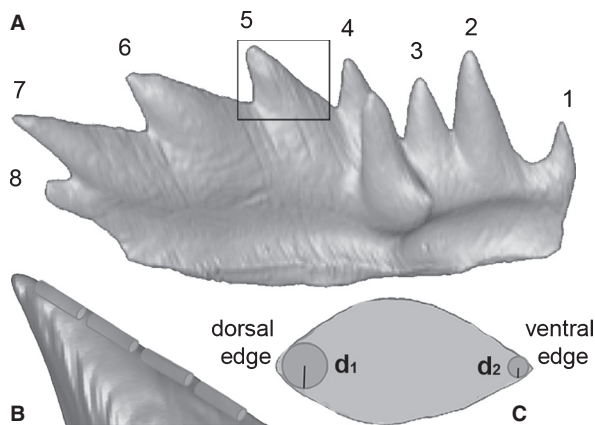


Fig. 3. Three-dimensional sharpness measurements of *Pseudofurnishius murcianus* P<sub>1</sub> denticles. A, the different denticles of the blade were identified and numbered from ventral to dorsal. B, to obtain more accurate values each denticle was divided in 4 equal intervals and measure individually, providing the mean of the best-fit cylinders for each interval a more realistic sharpness measures (see Jones *et al.* 2012). C, the sharpness of the dorsal and ventral edges of cusps and denticles was measured as the diameter of best-fit cylinders for each of the previous four sub-divisions of the length of the denticles' edges.

Microwear analyses of isolated P<sub>1</sub> elements of *Pseudofurnishius murcianus* were undertaken using a Hitachi S-4100 Scanning Electron Microscope hosted at the University of Valencia. All the isolated elements are deposited at the Museo de Geología de la Universitat de València (MGUV). The clusters studied are inventoried and catalogued in the micropaleontological collection of Geološki zavod Slovenije/Geological Survey of Slovenia (GeoZS).

The digital data sets for the pair of occlusal elements used in this study are available in the form of stereolithograph (stl) files that can be used directly in 3D printing, from the Dryad Digital Repository: <http://dx.doi.org/10.5061/dryad.nc4k0>. The full-volume srXTM data sets and models are freely available from the authors upon request.

## Results

### Element morphology

The P<sub>1</sub> elements of *P. murcianus* have been described in two different orientations, interpreting the platform as either an 'anterior' or a 'posterior' process. Based on comparative analysis of P<sub>1</sub> element morphogenesis in *P. murcianus* and its close relative *Sephardiella mungoensis*, Plasencia *et al.* (2010) argued that the platform is a development of the 'anterior' process, and not the 'posterior' process from which ozarkodinins usually develop. However, it is clear that the platform is neither, because it is effectively a compound of primary and secondary lateral processes. The 'anterior' and 'posterior' processes of ozarkodinins P<sub>1</sub> elements are invariably ventral and dorsal, respectively (Purnell *et al.* 2000; Donoghue *et al.* 2008).

P<sub>1</sub> elements of *Pseudofurnishius murcianus* are composed of a platform and free blades, which develop from an entirely blade-shaped element through ontogeny. The dorsal and ventral blades are composed of 5 to 13 denticles that are directed towards the cusp on the ventral process and away from the cusp on the dorsal process (Figs 1, 2C–F). The platform develops on the rostral side of the element, comprised of one to ten denticles, but showing great variability in their arrangement. The caudal side usually does not show any kind of ornamentation, but it is not uncommon to find 1 or 2 isolated denticles, rarely more, that in some instances constitutes a ridge (Fig. 1). There is a clear asymmetry in the morphology of the platforms of sinistral and dextral P<sub>1</sub> elements preserved within the articulated clusters, most particularly in terms of the num-

ber of denticles comprising the platform (the platform of the sinistral element bears fewer denticles) (Fig. 2C–F).

### Occlusion

Interactions between the  $P_1$  elements of *P. murcianus* were analysed through: (1) the direct observations of the clusters; (2) and using scale-enlarged three-dimensional prints of the elements to explore the physical interaction of the elements, before; (3) detailed modelling of occlusal kinematics within a digital environment.

In the clusters of  $P_1$  elements studied, as well as in those figured in the literature (Ramovš 1977, 1978; Krivic & Stojanovič 1978), the sinistral and dextral elements are occluded such that the rostral side of the sinistral element ('inner' in conventional descriptive terminology) is overlapped by the 'outer' caudal side of the dextral element (Fig. 2A,B), and the rostral lateral processes (the platforms) of both elements are usually interlocked (e.g. Ramovš 1978; pl. 1 figs 1–3; and Fig. 2G–I). Given that the elements are preserved in this occluded position in almost all of the clusters, we interpret this as reflecting an *in vivo* condition. We interpret the one cluster in which the elements are not preserved in this manner as reflecting post-mortem displacement.

The physical scale-enlarged three-dimensional prints of the  $P_1$  element pair preserved in one of the clusters allowed us to explore possible interactions between the elements (Fig. 4A). The opposing elements interlock with great stability, facilitated both by the parallel articulation of the opposing blades and the interdigitation of the rostral lateral processes that comprise the platform (Fig. 4A). In this position, very little relative motion is possible; the elements can pivot about the point of contact between their lateral processes but almost all of this motion requires the denticles of the dorsal processes to cross the soft tissue attachment surface of the opposing elements. The possible relative motion of the opposing elements in achieving occlusion is highly constrained, firstly by the dorsal and ventral blades, which limit movement within their plane and, subsequently, by the long denticles of the rostral processes of the platforms, which bring the elements into precise occlusion. This is achieved by a linear vector of motion approximately parallel to the plane of the element.

Occlusal analysis of the digital models bore out the inferences based on physical modelling alone, but afforded more detailed insight into occlusal morphology (Fig. 4B–L). The rostral lateral processes that comprise the platforms are the main

point of articulation, with the denticle of the primary lateral process on the sinistral element interdigitating between the two secondary processes of the dextral element (Fig. 4B). The denticles ventral to, and including the cusp, are comparatively small, facilitating interpenetrative occlusion of the dextral carina between the carina and the primary rostral 'inner' process of the sinistral element; the size of these denticles in the sinistral element is limited by occlusion with the primary caudal ('outer') process of the dextral element.

### Microwear and mesowear

Pristine  $P_1$  elements of *Pseudofurnishius murcianus* have denticles with sharp tips and a striate surface microtexture. Denticles of the blade show clear evidence of microwear, where the striate surface texture has been removed by smooth polishing on both sides of the blades (Fig. 5C,D,G). There is evidence of mesowear too, concentrated in the denticles of the rostral platforms, and on the tips of the denticles of the ventral part of the blade (those closest to the platform), where the tips of the denticles are rounded (Fig. 5C,E,F). In addition, spalls occur on both sides of the blade concentrated, in particular, on the ventral half of the element (Fig. 5A,B).

### Denticle sharpness

The denticles that form the blade are laterally (rostral-caudal) compressed, with the dorsal and ventral surfaces of the cusp and denticles narrowed to form sharp edges. We measured tip sharpness in a total of 26 denticles from four specimens (Table 1), of which 20 denticles have ventral edges that are sharper than their dorsal edges, although the differences are not significant (see Table 1).

## Discussion

### *The occlusal cycle of Pseudofurnishius murcianus P<sub>1</sub> elements*

Our occlusal analysis suggests that the approach angle of the occluding  $P_1$  elements of *Pseudofurnishius murcianus* was approximately orthogonal to their attachment surface (Fig. 4F–H). The dorso-ventral blade aligned the approaching elements and their occlusion was refined by the interdigitation of denticles in the lateral processes that comprise the platform. Some rotational movement is possible when the elements are occluded, but this would have been precluded *in vivo* because it requires that the denti-

cles pass beyond the attachment surface of the opposing element. The elements likely separated completely during each occlusal cycle, facilitating the ingress of food materials for processing and the egress of processed food materials. This occlusal hypothesis is supported by the independent analyses of microwear, mesowear and denticle sharpness.

Although the cusp and denticles exhibit evidence of *in vivo* wear, in the form of smooth polishing,

chipping and spalling, on the inferred non-occlusal surface (Fig. 5), this is always lighter than on the occlusal sides of the same denticles, and demonstrates both that occlusion was not always precise, and that the elements separated completely during the occlusal cycle. The smooth-polished surfaces on the occlusal side of denticles in the rostral platform and on those denticles of the blade closest to the platform are likely a consequence of element-on-ele-

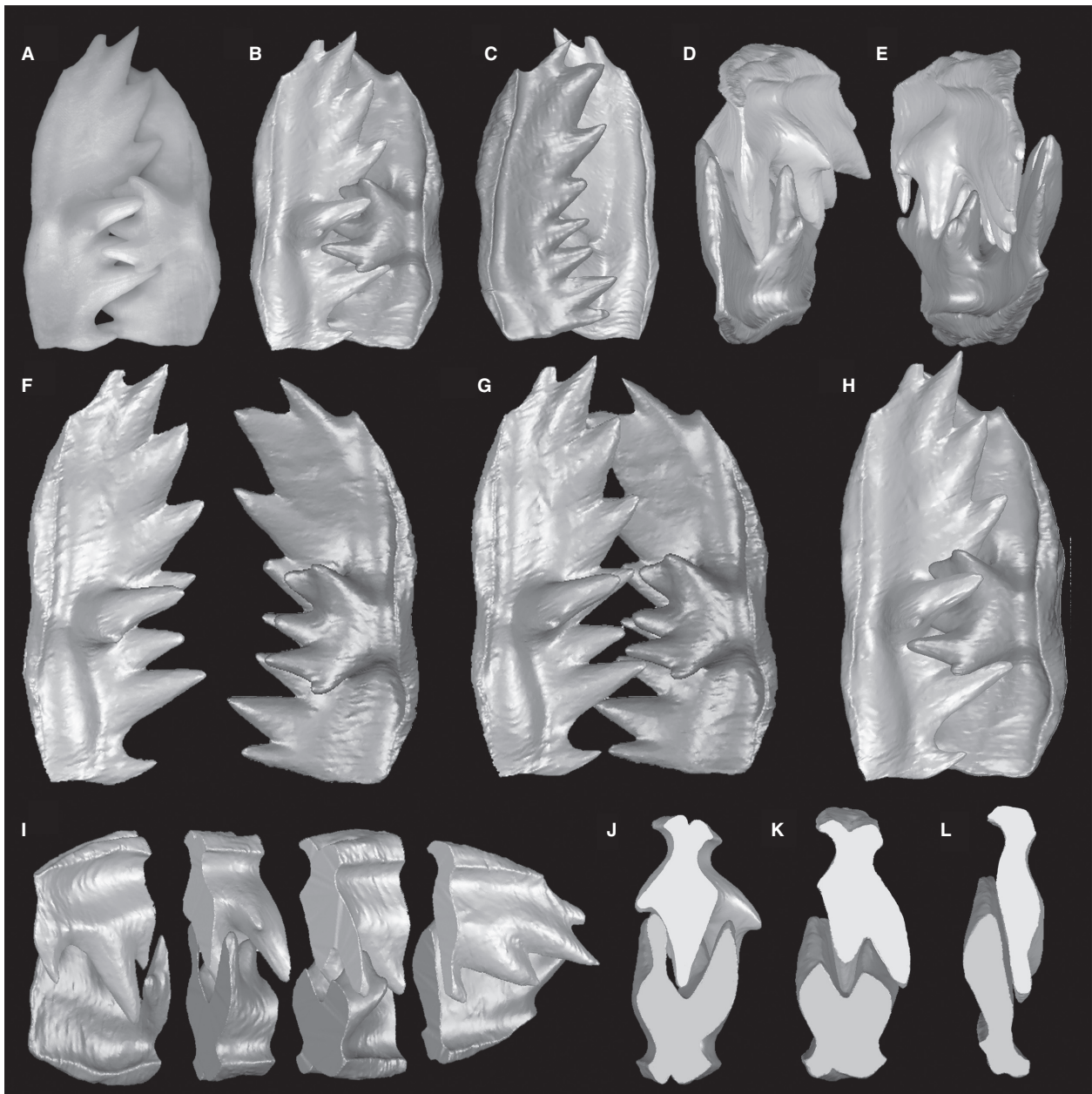


Fig. 4. *Pseudofurnishius murcianus* P<sub>1</sub> elements clusters from Prikrnica locality, Central Slovenia (GeoZS 559). A, scale-enlarged physical models of the elements from the articulated clusters for its physical occlusal analysis. B–E, digital occlusal model in its best constrained position, in rostral (B), caudal (C), ventral (D) and dorsal (E) views. F–H, Digital reconstruction of the occlusal cycle in rostral view with the opposed elements approaching approximately orthogonal to their attachment surface. I–L, serial digital sections to analysis the precise relation between the different structures of the opposite elements in the best constrained stage of the occlusal cycle, showing different sections from ventral (J) to dorsal (L). Models not to scale.

ment contact, rather than element-food contact, because these portions of the elements were responsible for guiding the final stages of approach of the occluding elements (Purnell 1995).

The clear asymmetry in the cross-sectional profile of the denticles supports our occlusal hypothesis because their marked flattening on the rostral 'inner' side of the sinistral element and on the caudal 'outer' side of the dextral element correlates with their sinistral-behind-dextral arrangement. The absence of any significant distinction between the sharpness of the dorsal and ventral edges of the denticles (see Table 1) supports our view that there is no rotational component to the occlusion cycle. Given that the dorsal edges of the denticles are approximately parallel to

the approach angle of the occluding elements, they presumably served largely to trap materials that were ultimately cut by the more obliquely aligned ventral edges of the denticles. Differences in the sharpness of the denticles, between the relatively sharp laterally compressed denticles of the dorsal process and the comparatively blunt denticles of the ventral and especially the lateral processes, reflect their functions in guiding occlusion and food processing, respectively.

#### Comparison to occlusal models for $P_1$ elements in other conodonts

Knowledge of conodont element occlusion is based on the  $P_1$  elements of few taxa. Analysis of

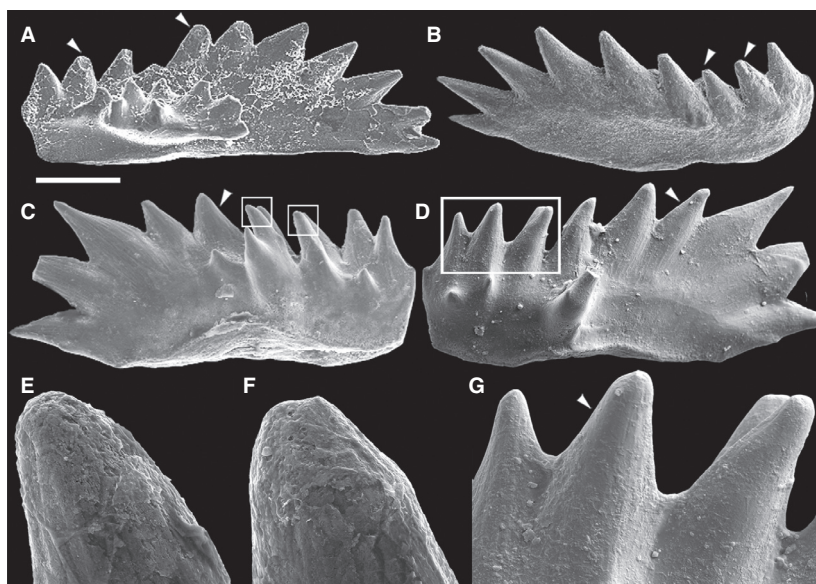


Fig. 5. Meso- and microwear in *Pseudofurnishius murcianus*  $P_1$  elements. A, left element showing spalls (white arrows) in its functional occlusal side (MGUV-10334, Calasparra, Murcia, Betic Ranges). B, left element showing spalls (white arrows) in its non-functional occlusal side (MGUV-10195, Henarejos, Cuenca, Iberian range). C–G, right element in rostral (C) and caudal (D) views, and enlarged areas (E–G), showing smooth polishing on blade and platform denticles on its occlusal (white arrows; C, E, F) and non-occlusal side (D, G). E, F, detail of the denticle platforms showing rounded tips and wear facets on its occlusal side. G, detail of smooth polishing in the denticles of the blade on the non-occlusal side (white arrows) (MGUV-10123, Calanda, Teruel, Iberian range). Relative scale bar: (A–D) 100  $\mu\text{m}$ ; (E, F) 16  $\mu\text{m}$ ; (G) 30  $\mu\text{m}$ .

Table 1. Mean and standard deviation (bracketed) for dorsal and ventral edges sharpness of *Pseudofurnishius murcianus*  $P_1$  elements from the Iberian Range (Bugarra section Spain) MGUV-21346 and MGUV-21247; and from the articulated pairs GeoZS 559 from the Prikrnica locality (Slovenia); see text for details. Values are missing where structures are broken or not well preserved.

	MGUV-21346 right element		MGUV-21347 right element		GeoZS 559 right element cluster		GeoZS 559 left element cluster	
	Ventral edge	Dorsal edge	Ventral edge	Dorsal edge	Ventral edge	Dorsal edge	Ventral edge	Dorsal edge
Denticle 8	–	–	6.1 ( $\pm 1.04$ )	7.48 ( $\pm 1.15$ )	–	–	–	–
Denticle 7	6.05 ( $\pm 3.55$ )	3.35 ( $\pm 0.69$ )	5.43 ( $\pm 0.66$ )	7.23 ( $\pm 1.67$ )	7.73 ( $\pm 1.47$ )	8.55 ( $\pm 2.33$ )	15.85 ( $\pm 5.95$ )	9.68 ( $\pm 2.76$ )
Denticle 6	5.66 ( $\pm 0.68$ )	5.95 ( $\pm 1.23$ )	6.28 ( $\pm 0.94$ )	8.13 ( $\pm 1.23$ )	9.28 ( $\pm 3.25$ )	7.8 ( $\pm 1.50$ )	13.63 ( $\pm 2.93$ )	16.1 ( $\pm 9.12$ )
Denticle 5	6.75 ( $\pm 0.77$ )	6.53 ( $\pm 0.71$ )	6.83 ( $\pm 1.14$ )	7.15 ( $\pm 1.70$ )	11.3 ( $\pm 2.83$ )	9.1 ( $\pm 0.2$ )	14.8 ( $\pm 0.97$ )	9.83 ( $\pm 1.60$ )
Denticle 4	7.05 ( $\pm 1.01$ )	9.08 ( $\pm 3.12$ )	7.03 ( $\pm 2.68$ )	9.85 ( $\pm 2.16$ )	9.73 ( $\pm 2.29$ )	11.63 ( $\pm 1.54$ )	6.85 ( $\pm 0.48$ )	8.95 ( $\pm 1.49$ )
Denticle 3	7.23 ( $\pm 1.36$ )	9.08 ( $\pm 2.50$ )	7.55 ( $\pm 2.36$ )	8.1 ( $\pm 1.16$ )	9.03 ( $\pm 1.63$ )	12.83 ( $\pm 3.04$ )	6.7 ( $\pm 2.21$ )	12.98 ( $\pm 4.41$ )
Denticle 2	7.53 ( $\pm 3.73$ )	8.58 ( $\pm 2.99$ )	6.85 ( $\pm 1.84$ )	7.83 ( $\pm 1.21$ )	17.85 ( $\pm 6.06$ )	18.48 ( $\pm 2.65$ )	8.63 ( $\pm 2.54$ )	10.23 ( $\pm 2.70$ )
Denticle 1	–	–	6.83 ( $\pm 1.59$ )	6.78 ( $\pm 0.66$ )	–	–	–	–

*Idiognathodus* inferred a rotational occlusal model in which the dorsal platforms and ventral blades of the elements occluded alternately, articulating about a complex of blade-parallel occluding ridges and troughs in the platform-blade complex of the opposing elements (Donoghue & Purnell 1999a). Rotational occlusion was implicated also for the blade-shaped P<sub>1</sub> elements of *Wurmiella*, although the elements were inferred to have separated completely as part of the occlusal cycle (Jones *et al.* 2012). Analysis of *Gnathodus* P<sub>1</sub> elements supported essentially the same pattern of rotational occlusion and evidence of microwear and spalling on the ‘non-occlusal’ sides of the elements indicated that the elements must have separated completely during phases of the occlusal cycle (Martínez-Pérez *et al.* 2014). Although all of these taxa exhibit rotational occlusion, their inferred power stroke is opposite; ventral to dorsal in platform elements and dorsal to ventral in blade-like morphologies (Donoghue & Purnell 1999a; Jones *et al.* 2012; Martínez-Pérez *et al.* 2014). It is entirely appropriate, therefore, that rotational occlusion has been considered general for P<sub>1</sub> elements (Martínez-Pérez *et al.* 2014).

Analysis of *Pseudofurnishius* P<sub>1</sub> elements demonstrates that, in comparison with *Idiognathodus*, *Wurmiella* and *Gnathodus*, differences in element morphology reflect differences in occlusal kinematics. *Pseudofurnishius* P<sub>1</sub> elements did not include a rotational component in their occlusal cycle but, rather, occluded approximately linearly, moving through a plane orthogonal to the element attachment surfaces. It is likely that differences in the geometry of the elements contribute to these differences in occlusal kinematics. Although the P<sub>1</sub> elements of the gnathodids and *Pseudofurnishius* all bear platforms, they differ in location (dorsal *versus* central) and in the manner of their development (lateral expansion of the dorsal process *versus* addition of primary and secondary lateral processes). The convex surfaces of the gnathodid platforms undoubtedly contribute to their pattern of rotational occlusion, although this occlusal pattern is seen also in the P<sub>1</sub> elements of *Wurmiella* which lack platforms. However, it appears that it is precisely the development of the lateral processes of the platform in *Pseudofurnishius* P<sub>1</sub> elements that restricts the relative movement of the elements to linear occlusion. Thus, these differences in the geometry of the elements may serve as a guide to interpreting their occlusal kinematics in other taxa where there is an absence of evidence from articulated remains.

Above all, this analysis of *Pseudofurnishius* P<sub>1</sub> elements and the novel morphology that they represent suggests that conodont element occlusal kinematics

are as disparate as element morphologies, supporting the view that there is no general model for occlusal kinematics in conodonts. Thus, the model species approach that has necessarily held sway in conodont dental functional analysis to date likely masks a greater diversity of feeding strategies than has been considered hitherto. Therefore, if we are to establish the role of this abundant and diverse, but hitherto overlooked, clade in Palaeozoic and Mesozoic marine ecosystems, there is a clear need to investigate occlusal kinematics in a manner that is more representative of the disparity of element morphotypes that are the staple of conodont classification schemes.

## Conclusions

Our functional analysis of *Pseudofurnishius murcianus* P<sub>1</sub> elements revealed a novel pattern of orthogonal occlusion distinct from rotational occlusal model described previously in all other functional analyses of conodonts (Donoghue & Purnell 1999a; Jones *et al.* 2012; Martínez-Pérez *et al.* 2014). It is likely that conodonts occlusal kinematics are as diverse as element morphotypes are disparate. Attempts to elucidate the diversity of occlusal kinematics and, therefore, feeding ecologies of conodonts will be repaid by an understanding of the role of this important abundant and diverse clade in Palaeozoic and Mesozoic marine ecosystems.

*Acknowledgements.* – The work was funded by Marie Curie FP7-People IEF 2011-299681 and postdoctoral fellowship from the Fundación Española para la Ciencia y la Tecnología (to C.M.P.). PP was supported by the Chinese Academy of Sciences (Young International Scientist Grant ‘2010Y2ZA02’) and by the ‘Agencia Española de Cooperación Internacional para el Desarrollo’ of the ‘Ministerio de Asuntos Exteriores y Cooperación (MAEC-AECID)’. The authors thank Dr. Federica Marone and Dr. Marco Stampanoni (Paul Scherrer Institute) for their help at the TOM-CAT beamline.

## References

- Donoghue, P.C.J. 1998: Growth and patterning in the conodont skeleton. *Philosophical Transactions of the Royal Society of London, Series B* 353, 633–666.
- Donoghue, P.C.J. 2001: Microstructural variation in conodont enamel is a functional adaptation. *Proceedings of the Royal Society of London, Series B* 268, 1691–1698.
- Donoghue, P.C.J. & Purnell, M.A. 1999a: Mammal-like occlusion in conodonts. *Paleobiology* 25, 58–74.
- Donoghue, P.C.J. & Purnell, M.A. 1999b: Growth, function, and the conodont fossil record. *Geology* 27, 251–254.
- Donoghue, P.C.J., Bengtson, S., Dong, X.-P., Gostling, N.J., Hultgren, T., Cunningham, J.A., Yin, C., Yue, Z., Peng, F. & Stampanoni, M. 2006: Synchrotron X-ray tomographic microscopy of fossil embryos. *Nature* 442, 680–683.
- Donoghue, P.C.J., Purnell, M.A., Aldridge, R.J. & Zhang, S. 2008: The interrelationships of ‘complex’ conodonts (Vertebrata). *Journal of Systematic Palaeontology* 6, 119–153.



- Dzik, J. 1991: Evolution of oral apparatuses in conodont chordates. *Acta Palaeontologica Polonica* 36, 265–323.
- Dzik, J. 2006: The Famennian ‘Golden Age’ of conodonts and ammonoids in the Polish part of the Variscan sea. *Palaeontologia Polonica* 63, 1–359.
- Jeppsson, L. 1979: Conodont element function. *Lethaia* 12, 153–171.
- Jones, D., Evans, A.R., Siu, K.K.W., Rayfield, E.J. & Donoghue, P.C.J. 2012: The sharpest tools in the box? Quantitative analysis of conodont element functional morphology. *Proceedings of the Royal Society of London, Series B* 279, 2849–2854.
- Krivic, K. & Stojanovič, B. 1978: Conodonts from the Triassic limestones at Priknica village (Konodonti v triadnem apnencu pri Prikrnici). *Geologija* 21, 41–46.
- Marone, F. & Stampanoni, M. 2012: Re-gridding reconstruction algorithm for real-time tomographic imaging. *Journal of Synchrotron Radiation* 19, 1029–1037.
- Martínez-Pérez, C., Donoghue, P.C.J., Rayfield, E.J. & Purnell, M.A. 2014: Finite elements, occlusion and wear analyses indicate that conodont microstructure is adapted to dental function. *Palaeontology*. doi:10.1111/pala.12102.
- Murdock, D.J., Sansom, I.J. & Donoghue, P.C.J. 2013: Cutting the first ‘teeth’ - a new approach to functional analysis of conodont elements. *Proceedings of the Royal Society of London, Series B* 280, 20131524.
- Nicoll, R.S. 1985: Multielement composition of the conodont species *Polygnathus xylus xylus* Stauffer, 1940 and *Ozarkodina brevis* (Bischoff & Ziegler, 1957) from the Upper Devonian of the Canning Basin, Western Australia. *Bureau of Mineral Resources Journal of Australian Geology and Geophysics* 9, 133–147.
- Nicoll, R.S. 1987: Form and Function of the Pa element in the conodont animal. In Aldridge, R.J. (ed.): *Paleobiology of Conodonts*, 77–90, British Micropaleontological Society series, Ellis Horwood, Chichester, Sussex.
- Plasencia, P. 2009. *Bioestratigrafía y paleobiología de conodontos del Triásico Medio del Sector Oriental de la Península Ibérica*, 408 pp. Servei de Publicacions de la Universitat de Valencia, Valencia, Spain.
- Plasencia, P., Hirsch, F. & Márquez-Aliaga, A. 2010: On the ontogeny and orientation of the Triassic Conodont P<sub>1</sub>-element in *Pseudofurnishius murcianus* Van den Boogaard, 1966. *Geobios* 43, 547–553.
- Purnell, M.A. 1995: Microwear on conodont elements and macrophagy in the first vertebrates. *Nature* 374, 798–800.
- Purnell, M.A., Donoghue, P.C.J. & Aldridge, R.J. 2000: Orientation and anatomical notation in conodonts. *Journal of Paleontology* 74, 113–122.
- Ramovš, A. 1977: Skelettapparat von *Pseudofurnishius murcianus* (Conodontophorida) in der Mitteltrias Sloweniens (NW Jugoslawien). *Neues Jahrbuch für Geologie und Paläontologie. Abhandlungen* 153, 361–399.
- Ramovš, A. 1978: Mitteltriassische Conodonten-clusters in Slowein, NW. Jugoslawien. *Paläontologische Zeitschrift* 52, 129–137.